

# **MEMS reliability for space applications by elimination of potential failure modes through testing and analysis**

Kin F. Man

Jet Propulsion Laboratory  
California Institute of Technology  
4800 Oak Grove Drive  
Pasadena, CA 91109

## **ABSTRACT**

As the design of Micro-Electro-Mechanical System (MEMS) devices matures and their application extends to critical areas, the issues of reliability and long-term survivability become increasingly important. This paper reviews some general approaches to addressing the reliability and qualification of MEMS devices for space applications. The failure modes associated with different types of MEMS devices that are likely to occur, not only under normal terrestrial operations, but also those that are encountered in the harsh environments of space, will be identified.

**Keywords:** MEMS devices, reliability, qualification, failure mode, test, analysis, modeling, space environments, mitigation.

## **1. INTRODUCTION**

Micro-Electro-Mechanical System (MEMS) devices have successfully been used in terrestrial applications for many years. Light-weight, low-cost, functionally-focused MEMS sensors and actuators promise to revolutionize space exploration in the next millennium. While the potential applications of MEMS are vast, the utilization of MEMS technologies in NASA's space missions have been limited thus far due to concerns of reliability and qualifiability of MEMS devices. Long-term reliability and survivability of MEMS devices for space applications require effective ground demonstration of reliable and robust operation in the hostile environment of space since they cannot be brought back to Earth for service. The establishment of qualification requirements and guidelines has been made difficult in part due to many types of MEMS devices, with different sets of failure modes stemming from different fabrication and construction techniques.

Most of the research on MEMS devices in the past couple of decades have focused on developing advanced fabrication techniques and improving their functional performance. It is only in the past few years when MEMS technologies and device performance have advanced sufficiently and the applications have become so critical that researchers have paid more attention to the issues of reliability and long-term survivability. The qualification of MEMS devices for reliable and robust operation in specific space environments has been one of NASA's prime focus.<sup>1,2</sup>

This paper focuses on the identification and understanding of the failure modes and mechanisms that can potentially occur in MEMS devices. The environments in which MEMS devices must survive for space applications will be presented. Tests, analyses, and modeling activities that can be performed throughout the development cycle to mitigate those failure modes will be described.

## **2. ENVIRONMENTAL TESTING**

Long-term reliability and survival of MEMS devices require effective demonstration of reliable and robust operation in the intended mission environment. The purpose of environmental verification and testing of a device is to demonstrate the quality and reliability of a design and its suitability for the intended application, and to screen for manufacturing workmanship defects. For space applications, the purpose is also to simulate the launch environment and to qualify the design for launch and operational conditions.

NASA's spacecraft can experience the most extreme of environments, those that are much more stringent than any commercial MEMS devices for terrestrial application could experience. For example, space MEMS devices could encounter acoustic noise of greater than 150dB from launch vehicles, temperatures ranging from 3K in deep space to almost 2000°C at

atmospheric entry, and acceleration forces of hundreds of thousands of g's on planetary surface impact. In addition, they could experience wide variations of high-energy particle irradiation fluxes, and pressure and vacuum levels. Testing for such extreme environments is therefore essential.

A space environmental verification and testing program typically involves a series of dynamic and thermal tests, which include pyroshock, acoustic noise, acceleration, random, and sinusoidal vibrations; and thermal-vacuum, thermal dwell, and thermal cycling. For devices that are sensitive to electromagnetic fields, an electromagnetic compatibility test should be conducted. Evacuated, sealed MEMS packages generally undergo a pressure leak test to ensure the integrity of the packaging. For MEMS devices operating in the radiation field of space, radiation testing is also recommended. This program should be designed to characterize the device for a specific application.

The following is a description of some typical testing for space environmental verification. The order in which the different tests are conducted should closely simulate the flight sequence. Experience has shown that the testing order does affect the effectiveness of screening for potential failures.<sup>3</sup>

Space MEMS need be tested to temperature levels commensurate with their exposure, typically at levels of  $-55^{\circ}\text{C}$  to  $70^{\circ}\text{C}$ , or  $\pm 20^{\circ}\text{C}$  of the flight allowable temperatures, whichever is the greatest. Thermal radiation from direct solar irradiation, reflected solar albedo, and planetary infrared radiation during Earth orbiting and deep-space cruising have to be taken into consideration.

The pressure a MEMS device in a spacecraft experiences decreases from atmospheric pressure on the surface of Earth to as low as  $10^{-6}$  torr. Devices should be designed accordingly, not only to ensure functional performance, but also to preserve structural integrity to prevent structural failure of the package.

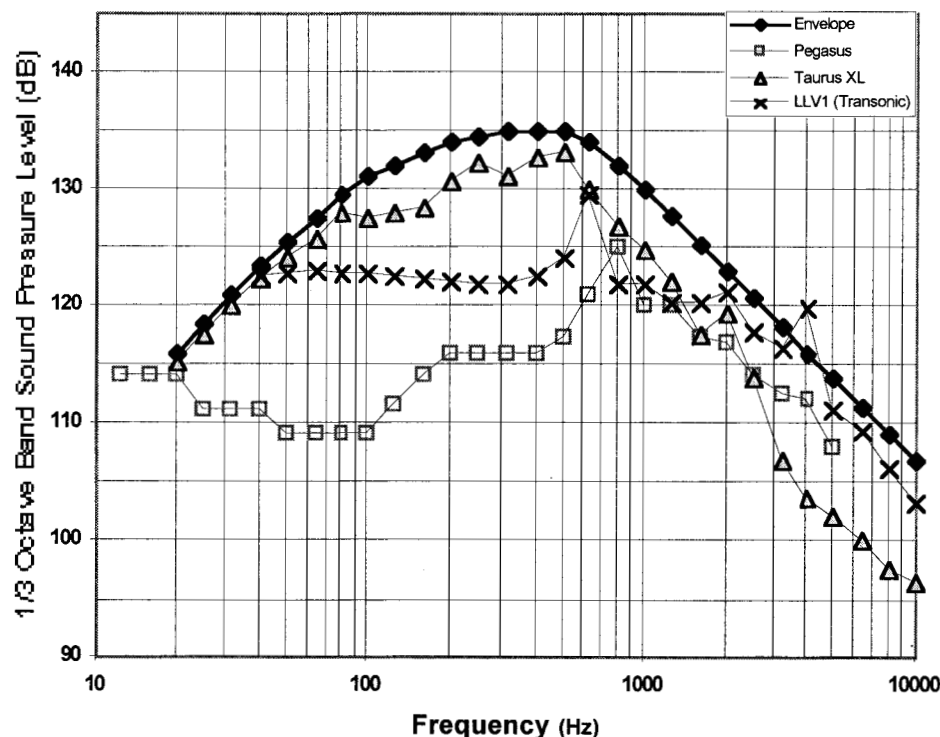


Figure 1. A plot showing acoustic flight data of 3 spacecraft and a test envelop<sup>4</sup>

Dynamic vibration and shock tests are performed to simulate the launch vibroacoustics and upper-stage pyrotechnic separation events. Sinusoidal vibration covers low to mid-frequency (5-100 Hz) launch vehicle-induced transient loading events. The random vibration test simulates launch vehicle-induced acoustic excitations during liftoff, transonic and maximum dynamic pressure events. Random vibration takes place over a broad frequency range, from about 10 Hz to 2000 Hz. In the space vehicle launch environment, random vibration is caused primarily by acoustic noise in the payload fairing, which in turn is induced by external aerodynamic forces due to dynamic pressure and reflection of rocket exhaust from the ground. The

acoustic noise test level is based on maximum internal payload fairing sound pressure level spectra. The fluctuating pressures associated with acoustic energy can cause vibration of structural components over a broad frequency band, typically in the range of 20 Hz to 10,000 Hz. Such high frequency vibration can cause structural fatigue. Figure 1 shows typical sound pressure levels as a function of frequency for three launch vehicles and an acoustic test envelope encompassing them for effective testing. The pyroshock test simulates the structurally transmitted transients from explosive separation devices, including pyrotechnic fasteners utilized to induce spacecraft separation from the upper stage. In addition, tests are also made to quasi-static accelerations associated with quasi-steady flight events from rocket motor-induced and other external forces which change slowly with time. Detailed test environmental specifications and levels are provided by Newell and Man.<sup>3</sup>

### 3. FAILURE MODES AND MECHANISMS

A failure is said to have occurred when a device or a system no longer performs the required functions under the stated conditions within the stated period of time. The performance encompasses both the mechanical behaviors of the sensor and the electrical characteristics of the entire system. There are two main categories of failures: (1) catastrophic (or irreversible) failures, which involves the total destruction of the device, rendering it completely inoperable, and (2) degradation failure, which consists of the device parameters operating far outside the normal range of operation. The latter can be either permanent or reversible, depending on the specific failure mechanism.

Failure modes usually refer to observable adverse effects (broken structure, cracked surface, jammed mechanism, etc.) or directly measurable parameter degradation exceeding the prescribed limits. Failure mechanisms are the processes directly causing the observable failure mode. Generally, there are more than one level of mechanisms, starting from one mechanism leading to another, eventually causing the observable failure mode. The term 'failure mechanism' is often used interchangeably with the term 'failure mode' to refer to all aspects of the failure process. Understanding the failure modes and mechanisms under different operational environments is a crucial part of addressing the issue of reliability, since mitigation strategies could be developed throughout the development and fabrication processes to ensure reliable operation of the device during the intended mission. A number of failure modes and mechanisms have been identified for MEMS devices.<sup>5</sup> The following sections provide a description of the primary failure modes, together with a discussion of the mitigation techniques to minimize them.

#### 3.1. Material Incompatibility

A number of materials are used for the construction of MEMS devices. Even before evaluation of the functional performance of a design, selection of the materials and their compatibility are the first considerations that determine the reliability of the device.

MEMS devices often use silicon and other electronic materials as mechanical structures. In addition to single crystal silicon, polycrystalline silicon (polysilicon) of different impurity concentrations and grain structures is another common structural material used for MEMS fabrication. Silicon is a monocrystal, mechanically-strong material that does not show creep or exhaustion and is well-suited for MEMS elements requiring bending. Polysilicon is readily compatible with micromachining processes. Sputtered thin films and traces of various metals, such as aluminum, tungsten, platinum, and gold, are used as electrical conductors and wires. Both silicon dioxide and silicon nitride have traditionally been used for electrical and thermal isolation, masking, and encapsulation. Because of its chemical inertness and lower intrinsic stress, silicon nitride is generally preferred over silicon dioxide. Silica glass is also increasingly being used for this purpose. Other materials used primarily for electrical isolation are aluminum oxide and polyimide. In addition to these structural materials, there has been an increasing interest of the use of amorphous and diamond-like carbon films and diamond structures in MEMS devices.<sup>6</sup> The large wetting angles, low surface energies, and small adhesion forces of carbon films make them candidate materials for reducing stiction and friction forces at MEMS interfaces.<sup>7</sup>

Since MEMS devices combine traditional microelectronic technologies with mechanical, electrical, and structural elements, the diversity of materials integrated together is likely to generate different failure modes from traditional microelectronics or from mechanical systems. Few studies have been conducted on the long-term stability of the materials used in MEMS devices. The materials and the processes that are widely used in electronics technologies are now required to fulfill different functions for MEMS devices. As an example, polysilicon is a material commonly used for MEMS devices, but reliable mechanical data is not available for devices that have dimensions on the order of microns. Properties such as Young's modulus and strength are uncertain because the device size often approaches the grain size of the material. There are simply insufficient grains in the substrate for random orientation to cause the material to be isotropic. The mechanical properties of micron-size polysilicon depend largely on the individual production lot and any test measurements would result in material properties data with large deviations.

Furthermore, techniques used to operate optical MEMS components, such as lenses, mirrors, optical switches, beam splitters, gratings, etc. often rely upon the electrostatic deformation of a mechanical membrane, beam, or cantilever to manipulate the optical beams. Micromirrors designed to use for optical switches, displays, and scanners, are examples of this.<sup>8</sup> They are made with thin metal films of aluminum and polysilicon. The main problem associated with fabricating membrane, beam, or cantilever mirror structures with metal or dielectric thin films has been the magnitude and variance of the stress generated in the materials during fabrication. When the mirrors are released, the internal stress causes them to bend in a concave or convex manner, depending upon the stress state (whether it is tensile or compressive) within the material. For micro-optical applications where surface flatness and uniformity are paramount, this problem is a severe impediment to the advancement of this device.

### 3.2. Fracture and Fatigue

Fracture occurs when the load on a device is greater than the strength of the material. Fracture is a serious reliability concern, particularly for brittle materials, since it can immediately or would eventually lead to catastrophic failures. Additionally, debris can be formed from fracturing of microstructures,<sup>7</sup> leading to other failure processes. For less brittle materials, repeated loading over a long period of time causes fatigue that would also lead to the breaking and fracturing of the device. In principle, this failure mode is relatively easy to observe and simple to predict. However, the fatigue properties of thin films are often not known, making fatigue predictions error prone. There are several ways to avoid fracture failure from occurring. One approach is to design the device with the maximum applied stress safely below the stress at which failure occurs or use a material that has a material strength far exceed the maximum stress expected. Unfortunately, the mechanical properties of materials required for the design of reliable MEMS devices are often not well understood or unavailable at the microscopic level.

A knowledge of the mechanical properties at the microscopic level is therefore highly desirable. These data are often unavailable. At the macroscopic level, mechanical properties are often measured using tensile stress tests. Such tests are difficult at the microscopic level because there is no accurate method of measuring the applied forces at the sizes involved. Consequently, multiple tests using many samples to obtain statistically meaningful data would likely result in significantly different values of Young's modulus.

Bromley et al.<sup>9</sup> proposed a method for using experimentally measured data that accounts for the uncertainties in mechanical properties. Their method involved loading the test elements with a specified displacement rather than a force and ensuring that the displacements were large enough to be accurately measured optically. For this arrangement, assuming that the Young's modulus is a constant, the strain may be calculated without knowing the Young's modulus of the material and the same strain result regardless of the magnitude of it. Each device was loaded until it fractured, the displacement at fracture was measured and the associated strain was calculated using a commercial finite element analysis program capable of non-linear analysis. Measurements were made on polysilicon which is a brittle material and is assumed to fracture without going into a non-linear stress-strain regime. They tested 161 microdevices to failure, and recommended that the nominal strain be maintained below 0.0055 for future design of polysilicon MEMS devices.

### 3.3. Adhesion and Stiction

Thin film micromechanical structures made by surface micromachining and deposition techniques are commonly found in many MEMS devices.<sup>10</sup> They often include smooth and chemically active surfaces. Their dimensions are typically 50 to 500  $\mu\text{m}$  in the lateral direction and thicknesses of 0.1 to 3  $\mu\text{m}$  with a separation of only 0.1 to 2  $\mu\text{m}$  away from the substrate. Due to large surface area to volume ratio in surface microstructures, they are particularly prone to adhesion (also known as stiction) to the substrate or nearby structures when they are bent unintentionally due to dynamic disturbance or intentionally as part of normal operation.<sup>11,12</sup> For devices with surface actuation motions in the normal direction or having sliding contact, friction and wear are also critical concerns<sup>13</sup> which will be discussed in the next section.

Komvopoulos<sup>7</sup> described various surface stiction mechanisms, such as solid bridging, capillary force from liquid meniscus formation, van der Waals force, and electrostatic charging, and the effect of surface roughness. Different methods of reducing adhesion and stiction by modifying the structural stiffness, interfacial topography, and surface chemistry characteristics were also discussed. Experimental and theoretical results for the stiffness of silicon micromachines needed to overcome stiction were compared for different surface roughness. Based on those results, the efficacy of different surface engineering techniques, such as formation of standoff bumps on one of the countersurfaces, roughening or texturing, and surface chemistry modification (e.g. self-assembled monolayers), to reduce high adhesion forces at MEMS interfaces was interpreted. Surface

engineering and modification of physiochemical surface properties were shown to be effective in enhancing the reliability and performance of microdevices.

Although surface modification to reduce the surface energy through chemical treatments or lubrication was shown to be an effective method of reducing adhesion and friction, MEMS fabrication processes themselves pose stringent constraints on the surface coatings that can be applied. The challenge is to create coatings that are compatible with the fabrication process, as well as with the eventual die attachment and device packaging. In order to make the coatings effective, it is important to understand the properties of the materials used in MEMS fabrication and the interfacial forces responsible for stiction in microdevices.

Permanent adhesion arises from the large interfacial forces compared with the restoring force of the deflected structure. As mentioned above, these include capillary, electrostatic, and van der Waals forces. (Since the dimensions of most microdevices are minute, gravity and other body forces do not play a significant role.) All of these forces must be manipulated if the adhesion force is to be reduced below the spring restoring force. An effective treatment for these microstructures must provide a stable hydrophobic surface in order to avoid the formation of water layers on the surface, thereby eliminating capillary forces altogether. The removal of the hydrophilic hydroxyl groups from the surface will also eliminate the possibility for hydrogen bonding as the two surfaces come into contact.<sup>14</sup> To minimize electrostatic attraction, the two surfaces should be conductive, allowing charges to be dissipated. A reduction in the effective contact area is also necessary to further reduce the overall adhesion forces in microdevices.

Reducing the contact area between adjacent surfaces by roughing the surface on a microscopic scale or by fabricating microdimples were initially attempted for polysilicon to reduce adhesion. However, polysilicon surfaces, as deposited and annealed, are rather rough, with root-mean-square (rms) values in the range of a few nanometers to a few 10's of nanometers.<sup>15</sup> As such, additional surface roughening alone was found to have limited effect on reducing adhesion during operation. Although some improvements were observed due to roughening, chemical surface modification of the polysilicon was found to be more effective.<sup>14</sup>

A number of experimental techniques have been developed specifically to examine the surface-to-surface interactions involved in silicon microstructures with a goal of quantifying adhesion between two microstructures and determining the coefficients of friction between two surfaces. Maboudian<sup>14</sup> reviewed various experimental designs used to quantify adhesion and friction in the length scale relevant to MEMS technology.

### 3.4. Friction and Wear

Many MEMS devices involve surfaces contacting or rubbing against one and other, leading to friction and wear.<sup>13</sup> The operation of micromachined devices that have contacting joints and bearings is significantly affected by friction and wear of the contact surfaces involved. Gabriel et al.<sup>16</sup> have observed significant wear on the hub of a micromotor. In a micromotor, the rotor is driven electrostatically in the stator, but in practice because of the small clearance between the hub and rotor, there may be some physical contact. Reducing the friction at the hub/rotor interface is critical for high-speed performance. Friction and wear properties of materials used in the fabrication of contact surfaces must be improved for the long-term reliability and high performance.

Adhesive wear occurs when elements in a device rub together causing small pieces to rip off. These pieces attract and stick to each other, particularly in high-humidity environments, resulting in regions where micromachines get jammed up and fail. Adhesive wear was found to be a major contributor to MEMS failures. Abrasive wear is a cutting or material removal of the surface increasing its roughness. Failures due to adhesive and abrasive wear have been identified in MEMS comb drives and microengines under normal operations.<sup>17,18</sup> Microwelds, which are a fusion of two surfaces at the contact points of the two surfaces, can increase friction permanently if the contacts are large. Increased friction would affect the performance of a comb drive or other actuator surfaces.

Silicon is a widely used material for MEMS fabrication. However, friction and wear properties of silicon may not be adequate for many sliding applications. The mechanical and tribological properties may have to be improved to meet the functional performance and reliability requirements. One method to improve mechanical properties and possibly tribological properties is by ion implantation. Ion bombardment of crystalline silicon creates damage. It amorphizes and modifies the chemical composition of the crystals by forming compound layers in the near surface region. Ion beam synthesis which involves the implantation at high doses of energetic ions into single crystal silicon at high temperatures has been successfully used to achieve a variety of buried compound layers in silicon. However, the tribology of bulk and thin films of single-crystal and polycrystalline silicon is not well understood. Braun et al.<sup>19</sup> reported a drastic reduction in the coefficient of friction of single-

crystal silicon after the deposition of thin carbon film post bombarded by  $N^+$  and  $C^+$  ions. Gupta et al.<sup>20</sup> reported that  $C^+$  implanted silicon exhibits very low coefficient of friction and low wear, while slid against steel and alumina in dry and moist air, and dry nitrogen atmospheres. The ion implantation apparently resulted in the formation of layers of SiC, C and Si on the surfaces which caused the reduction in wear.

Single-crystal and polycrystalline silicon wafers have also been implanted with boron ions to improve their mechanical and tribological properties.<sup>20</sup> The effects of ion implantation on the crystallinity, microstructure, nanohardness, friction, and wear properties were studied and it was found that silicon remained crystalline after ion bombardment at doses up to  $2 \times 10^{17}$  ions.cm<sup>-2</sup> but with a large amount of defects. It was also found that there was a small increase in the nanohardness due to boron-ion implantation and the ion-bombarded single-crystal silicon exhibited very low friction and low wear factor. The coefficient of friction of bombarded silicon in dry air and dry nitrogen was found to be even lower. The coefficient of friction and wear factor of silicon bombarded at high doses were measured to be lower at low humidity and dry nitrogen than at high humidity. The fracture of silicon surface and its oxidation during sliding were believed to play a significant role in the friction and wear process. Ion implantation generally improves friction and wear properties of surfaces, but the benefit depends on the operational environments.

### 3.5. Electrostatic Interference

Materials of extremely high insulation resistance and breakdown field strength, such as silicon oxide and silicon nitride, are often used for insulation in MEMS devices and as part of electrostatically driven actuators and capacitive sensors. Some sensors also use these dielectrics as very thin elastic diaphragms. The surface of such dielectrics can be charged up locally and the charge retained for a considerable time under certain conditions. Sometimes they provide trap sites for positive and negative charges both deep in the volume and at the interfaces in multilayer stacks. Electrostatic charging effects are of great importance to micromachines as they can be a significant fraction of the total normal force applied to a mechanical contact.<sup>7</sup> Stray charge accumulation on the dielectrics of sensor and actuator devices inevitably distort the electric field and change the device characteristics.

Charging can arise during handling and operation. In a stacked oxide-nitride dielectric of polysilicon comb drives,<sup>22</sup> such undesirable charging effects originate from the electron beam of the scanning electron microscopy used for device testing. Once fabrication is completed, two major electrophysical effects can lead to the presence of parasitic charges in MEMS elements besides e-beam charging. First, contact electrification occurs due to mechanical surface contact of two materials with different work functions and their subsequent separation. This phenomenon may be observed at pull-in of electrostatically actuated parts. Gas discharges with the capacitive air gap is the second origin of charging.<sup>22</sup> High operating voltage exceeding the breakdown voltage of the gap leads to considerable charge deposition of the dielectric layers. Even if the dimensions are designed for operating voltages not exceeding the air breakdown voltage, static electrification in common handling environments can cause dramatic voltage buildup of several kilovolts. Wibbeler et al.<sup>22</sup> have investigated the impact of parasitic surface charges on the deflection versus voltage characteristics of bulk micromachined silicon cantilever actuators and presented measurements of the charge decay. They also provided a comparison between the electrostatic forces induced by parasitic charges and practicable detection forces in sensor applications.

Dielectric layers used for short-circuit protection in capacitive MEMS are unable to eliminate the risk of gas discharges between the insulated electrodes.<sup>22</sup> Gas breakdown has been observed for silicon cantilever actuators due to operation at several hundred volts, even though the aluminum electrodes were covered during passivation. Accumulation of the generated free electrons and ions at the dielectric surface was the cause of the failure. The parasitic surface charge led to an offset error seen in the deflection versus voltage curve of the device, causing an erroneous output. Meunier et al.<sup>23</sup> performed accelerated aging tests of a commercial micro-accelerometer and found a failure of the device due to irreversible electrostatic sticking between the movable cantilever beam and the fixed cantilevers as a result of excessive voltage applied to the center plate.

In addition to proper dimensioning of air gaps and operating voltages to exclude gas discharges during operation, precautions to protect capacitive microdevices from static electrification by an array of small insulation dots can be an effective means for reducing the chargeable surface and for speeding up the charge decay.<sup>22</sup> A long-term solution would be to replace the dielectric material with one that would dramatically reduce the charge decay time.

### 3.6. Radiation Damage

Traditional microelectronic devices are known to be susceptible to radiation damage. MEMS devices that are activated by electric fields across insulators are likely to be affected by high energy radiation effects through similar mechanisms. Although few studies have been made on the effects of radiation on MEMS, all the available results indicate similar potential problems,



such as single event dielectric rupture or bulk lattice damage leading to material rupture. Electrostatic attraction and friction can potentially be aggravated by charging effects. Radiation-induced charging may enhance or contribute to microwelding, electrostatic clamping, or wear processes between two surfaces where small gaps or contacts occur. In a microengine, sub-micron gaps exist between gear hub and drive gear, and gear pin and drive gear. A significant radiation-induced charging potential between polysilicon layers may be developed at these locations.

Two different MEMS acceleration sensors, fabricated with surface micromachining techniques, have been characterized for their total dose radiation response to ionization radiation.<sup>24</sup> Different failure mechanisms were observed when the sensor element or the whole device was irradiated. Even though the design of the sensor components was similar, the sensitivity to total dose radiation was quite different due to the technology difference of the supporting electronic circuits. The BiCMOS sensor functioned at much higher radiation levels than the CMOS sensor. The sensor with a BiCMOS structure integrated circuit was more tolerant to total dose irradiation. Localized irradiation also revealed that the BiCMOS sensor element was affected by radiation, as well as the peripheral electronics. This might have been caused by charge build-up in the oxide under the polysilicon sensor structure. Low dose-rate tests did not change the failure level of the CMOS device. It appeared that the CMOS output circuitry of the device was the primary cause of failure.

When the mechanical (sensor) part of two MEMS accelerometers was exposed to protons and heavy ions, Knudsen et al.<sup>25</sup> observed large changes in the measured acceleration outputs for one type of accelerometer and very little changes to the other type. The large voltage shift for the former was attributed to charges generated by the ions and trapped in dielectric layers below the mechanical arms which formed the moving plates of two variable capacitors. The trapped charges altered the electric field distribution around the capacitor which, in turn, led to changes to the output voltage. The construction of the latter device was such that the dielectric layers were covered with a conducting polysilicon layer that effectively screened out the trapped charges, leaving the electric field around the mechanical arms, hence the output voltage unchanged. Charge trapping in dielectric layers was found to degrade the performance of the sensor. These results suggest that, in trying to understand the origins of MEMS sensitivity to radiation, it is important to consider mechanical sensor construction and device architecture, particularly if the mechanical sensor is part of an integrated circuit.

Schanwald et al.<sup>17</sup> evaluated the mechanical and electrical performance of MEMS comb drive and microengine actuators in the total dose radiation environments. Comb drives are reciprocating linear electrostatic devices, a key element of MEMS microengine. Interdigitated comb teeth create the electrostatic force to induce the linear motion. Individual comb drives and microengines were evaluated as mechanical units to assess the effects of irradiation on their mechanical and electrical response. Two types of operational failures were found for comb drives, (1) lateral (adjacent comb teeth) electrostatic clamping and (2) linear (comb teeth at end of travel) electrostatic clamping. The lateral forces between interdigitated comb teeth should cancel out, but they sometimes become unstable. The end-line forces at the tips of the teeth are added to create the net force. This net force moves the teeth in attraction only along the teeth length for any polarity net voltage difference. The force does not depend on the relative lengthwise position between the teeth and is constant for a constant voltage difference. These failures can be aggravated by radiation effects.

Radiation sensitivity for a microengine drive gear depends on three electrical bias conditions: floating, grounded, and power on during irradiation. A common failure mode observed for ungrounded comb drives was linear and lateral clamping as described above. Another observed radiation effect was an increase in displacement of comb drive in a non-grounded bias arrangement, and to a much lesser degree for grounded elements. This increase in displacement was the only other effect observed that was unique to radiation. One likely cause of increased displacement was an additional force introduced to the comb-drive force balance by an unshielded strip of exposed nitride at the end of travel for the comb teeth. This effect may be reduced by decreasing the exposed nitride strip width. Another possible cause of increased displacement under electron and proton exposures is ion displacement effects producing spring fatigue.<sup>17</sup>

### 3.7. Thermal Effects

Many MEMS devices operate near their thermal dissipation limit. They may encounter hot spots that may cause failures, particularly in weak MEMS structures, such as diaphragms or cantilevers. Mismatched thermal expansion coefficients can also cause interface failures. The miropump,<sup>26</sup> consisting of a silicon diaphragm and a heater unit made of a resistor deposited on an alumina substrate, contains many different materials. The main problem stems from the mismatch of the coefficient of thermal expansion (CTE) between the molding compound and the other materials. This mismatch induces thermomechanical stresses and strains within the packaged device, particularly at the interfaces during temperature cycles and the post molding cool down of the assembly. Such repetitive stress can ultimately lead to fatigue failure. The induced stress and strain can damage the silicon diaphragm as well as the electronic chips. Pellet et al.<sup>26</sup> have evaluated the thermomechanical stresses

inside the assembly by thermal cycling from -50 °C to 150 °C and by finite element simulations. The results indicated that appropriate selection of materials was the primary factor in improving reliability.

The buried silicon-dioxide layer in silicon-on-insulator (SOI) circuits has a very low thermal conductivity, which results in large thermal resistance between the device and the chip packaging. This is a major problem for transistors that experience brief pulses of heating, such as ESD protection devices, for which the temperature rise is dominated by conduction within microns of active regions. Good lateral conduction parallel to the plane of the wafer in the silicon device layer can strongly reduce the local temperature rise and over heating in active regions.

#### 4. MODELING AND COMPUTER ANALYSES

Analytical techniques and mathematical calculations have been used to analyze relatively simple MEMS elements. As the design of MEMS devices become more complex, computer models and finite element analyses are necessary to fully understand the device characteristics. Finite element analyses provide an accurate method of predicting the temperatures, stresses, and dynamic responses of the entire structure. Furthermore, computer models and finite element analyses are convenient tools for characterizing the device functional performance before the expensive and time-consuming fabrication and testing processes even begin, thus allowing the design to be optimized early in the development. These tools have been used in a number of wide ranging applications, some of which are described below.

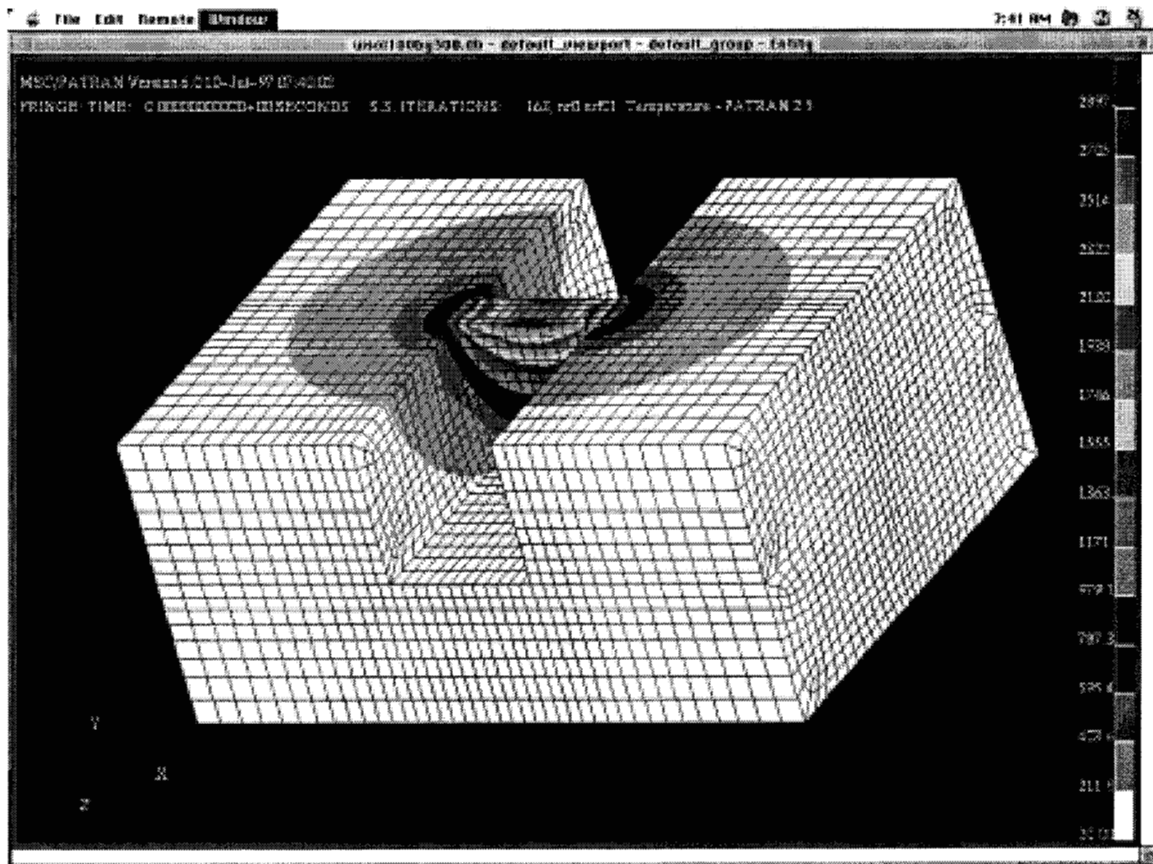


Figure 2. A computer model displaying the temperature distribution around the channel barrier<sup>27</sup>

Forgrave et al.<sup>27</sup> used finite element analysis to assist in the design and development of the microisolation valve. The small, electrically-actuated, one time-opening valve for turning on small flow of pressurized gasses was analyzed and characterized by finite element analysis. This MEMS-based valve, fabricated mostly from silicon, was designed to replace the larger pyrotechnically actuated valve. A channel was etched into the silicon substrate with a doped silicon plug placed at one location along the channel to obstruct flow. The valve was opened by supplying a sufficient amount of electrical power, via a deposited conductive trace, to melt or vaporized the plug by resistive heating. Finite element analysis was conducted on different silicon thicknesses to model the transient heat profile as the actuation current is applied, and to obtain a thermally



induced stress profile from the heating. The thermal steady state results were used to determine the amount of power required to melt the silicon barrier. Figure 2 shows the temperature distribution around the channel barrier with an applied input power.

Depth-sensing indentation (nanoindentation) is one method of characterizing the mechanical properties of materials. As the thickness of material films decreases, obtaining a substrate-independent measure of the mechanical properties of layers becomes increasingly difficult because of the influence of the substrate material. The problem is worse for implantation-modified surfaces, since the properties of a layer may vary through its depth. Knapp et al.<sup>28</sup> have developed a finite-element modeling procedure to reliably extract mechanical properties for thin, hard films and ion-modified layers on softer substrate. The method deduces the yield stress, Young's modulus, and hardness from indentations as deep as 50% of the layer thickness to an accuracy of within 10%. Two hard material layers, Ti- and C-implanted nickel, and diamond-like carbon layer which is potentially useful for reducing friction and wear, were evaluated. It was shown that the modeling was applicable even for materials whose hardness approaches that of diamond.

Applied electric fields produce traction on the surfaces of MEMS structures, such as plates, shells and beams, and cause them to deform. The shape distortion changes the capacitance of these structures and this, in turn, changes the forces on them. The simulation of MEMS elements involves computing the deformations and stresses in the structure when subjected to electric fields and electrostatic forces. Shi et al.<sup>29</sup> have conducted simulation of the coupled electromechanical behaviors of MEMS. Their computational methodology was based on coupling an exterior boundary element method for electrostatics with a finite element method for elasticity. The numerical procedures were applied to the simulation of a tungsten microtweezer, a conceptually simple MEMS device with nonlinear behaviors. Their goal was to develop simulators to enable a better understanding of MEMS behaviors, and to assist in the design and fabrication of optimal MEMS structures. A key feature of this methodology was the iterative design process involving simulation, sensitivity analysis, and optimization.

Five types of micromirror arrays have been designed and fabricated using the three-level polysilicon surface-micromachined fabrication technology.<sup>8</sup> The electrostatically deflectable micromirror designs include arrays of simple cantilever beams, torsion beams, tethered beams, circular membranes, and oval membranes. Modeling has been performed to investigate the microdynamic behavior of the torsion beam micromirror because it manifested the unique characteristic of possessing both in-plane and out-of-plane motion. The IntelliCAD<sup>30</sup> finite element analysis MEMS software program was used to verify the step-by-step fabrication of the torsion beam micromirror design and to generate the data for a plot of micromirror deflection versus applied voltage. Reliability tests on each micromirror design revealed that the large circular membrane and oval membrane micromirror designs failed after they had been cycled more than 1 million times. The simple cantilever beams, torsion beams, and tethered beams were tested in excess of 2 million cycles, and no failures were observed. These results supported the validity of the model calculations.

## 5. CONCLUSIONS

The acceptance of MEMS devices for space and critical applications depends largely on their reliability. In this paper, the predominant failure modes of MEMS devices operating in different environments have been identified. Many tests and analyses that can be performed to understand their failure mechanisms are described. Also described in this paper are mitigation techniques that have been developed to eliminate failures during different phases of the development and fabrication processes, thus increasing their reliability and qualifiability for space and critical applications.

## 6. ACKNOWLEDGEMENTS

The work described in this paper was conducted at the Jet Propulsion Laboratory, California Institute of Technology, under contract with the National Aeronautics and Space Administration (NASA). It was funded by NASA Code Q as part of the Payload Assurance Program. The author would like to thank S. Cornford, T. Larson, S. Kayali, B. Stark, R. Ramesham, J. Newell, J. Forgrave, S. Bolin, R. Lawton, W. Tang, and A. Wallace for their support and collaboration in these activities.

## 7. REFERENCES

1. A. P. Wallace, K. F. Man, and J. Mueller, "A Physics-of-Failure Based MEMS Qualification Methodology and its Application to the Vaporizing Liquid Microthruster," Proceeding of the MEMS Reliability and Qualification Workshop, Jet Propulsion Laboratory, Pasadena, California, August 5, 1997.
2. B. Stark, J. Bernstein, D. Gerke, S. Kayali, T. Kenny, K. Man, J. Newell, and W. Tang, "MEMS Reliability and Qualification Guidelines for Space Applications," Jet Propulsion Laboratory Internal Publication, D-16460, 1998.

3. J. M. Newell and K. F. Man, "Environmental Testing of MEMS for Space Applications," Proceeding of the MEMS Reliability and Qualification Workshop II, Pasadena, California, August 4-5, 1998.
4. J. M. Newell, "Acoustic Noise Requirements," pp5-9, *Risk/Requirements Trade-Off Guidelines for Faster, Better, Cheaper Missions*, Kin F. Man, Editor, Jet Propulsion Laboratory Internal Publication, D-13277, Rev. E, Feb 1998.
5. K. F. Man, B. H. Stark, and R. Ramesham, "A Resource Handbook for MEMS Reliability," Jet Propulsion Laboratory Internal Publication, D-16171 Rev. A, Dec 1998.
6. R. Ramesham, "Fabrication of Diamond Microstructures for Microelectromechanical Systems (MEMS) by a Surface Micromachining Process," *Thin Solid Films* **340**: (1-2) 1-6 FEB 26 1999.
7. K. Komvopoulos, "Surface Engineering and Microtribology for Microelectromechanical Systems," *WEAR* **200**: (1-2) 305-327, Dec 1996.
8. E. S. Kolesar, P. B. Allen, J.W. Wilken, and J. T. Howard, "Implementation of micromirror arrays as optical binary switches and amplitude modulators," *Thin Solid Films* **332**: (1-2) 1-9, Nov 2 1998.
9. S. C. Bromley, L. L. Howell, B. D. Jensen, "Determination of maximum allowable strain for polysilicon micro-devices," *Eng Fail Anal* **6**: (1) 27-41 Feb 1999.
10. W. S. Trimmer, *Micromechanics and MEMS, Classic and Seminal Papers to 1990* (IEEE Press, New York, 1996).
11. R. Maboudian and R. T. Rowe, "Critical review: Adhesion in surface micromechanical structures," *J. Vac. Sci. Technol. B*, **15**, 1-20, 1997.
12. C. H. Mastrangelo, *Tribology Lett.* **3**, 223, 1997.
13. S. Henck, *Tribology Lett.* **3**, 239, 1997.
14. R. Maboudian, "Adhesion and Friction Issues Associated with Reliable Operation of MEMS," *MRS Bull.* **23**: (6), 47-51, 1998.
15. M. R. Houston, R. T. Rowe, and R. Maboudian, "Effect of hydrogen termination on the work of adhesion between rough polycrystalline silicon surfaces," *J. Appl. Phys.* **81**, 3474-3483, 1997.
16. K. J. Gabriel, F. Behi, and R. Mahadevan, "In-Situ Friction and Wear Measurements in Integrated Polysilicon Mechanisms," *Sensors and Actuators*, **A21-23**, 184-8 1990.
17. L. P. Schanwald, J. R. Schwank, J. J. Sniegowski, D. S. Walsh, N. F. Smith, K. A. Peterson, M. R. Shaneyfelt, P. S. Winokur, J. H. Smith, and B. L. Doyle, "Radiation Effects on Surface Micromachined Comb Drives and Microengines," *IEEE Trans Nucl Sci* **45**: 2789-2798 Part 1 Dec 1998.
18. D. M. Tanner, W. M. Miller, W. P. Eaton, L. W. Irwin, K. A. Peterson, M. T. Dugger, D. C. Senft, N. F. Smith, P. Tanyunyong, and S. L. Miller, "The Effect of Frequency on the Lifetime of a Surface Micromachined Microengine Driving a Load," pp.26-35, *IEEE International Reliability Physics Symposium*, Reno, NV, March 30 - April 2, 1998.
19. M. Braun, H. Khosroupour, E. Johansson and S. Hogmark, "Formation and Characterization of Carbon Layers Deposited During Ion Bombardment of Silicon," *Nucl. Inst. Meth. Phys. Res.*, **B37/38**, 434-7, 1989.
20. B. K. Gupta, J. Chevallier and B. Bhushan, "Tribology of Ion Bombarded Silicon for Micromechanical Application," *J. Tribology*, **115**, 392-9 1993.
21. B. K. Gupta, B. Bhushan, and J. Chevallier, "Modification of Tribological Properties of Silicon by Boron Ion-Implantation," *Tribol T* **37**: (3) 601-607 Jul 1994.
22. J. Wibbeler, G. Pfeifer, and M. Hietschold, "Parasitic charging of dielectric surfaces in capacitive microelectromechanical systems (MEMS)," *Sensor Actuat A-Phys* **71**: (1-2) 74-80 Nov 1 1998.
23. D. Meunier, R. Desplats, J. Benbrik, G. Perez, C. Pellet, D. Etseve, and B. Benteo, "Electrical characterization and modification of a MicroElectroMechanical System (MEMS) for extended mechanical reliability and fatigue testing," *Microelectron Reliab.* **38**: (6-8) 1265-1269 Jun-Aug 1998.
24. C. I. Lee, A. H. Johnston, W. C. Tang, C. E. Barnes, and J Lyke, "Total Dose Effects on Microelectromechanical Systems (MEMS): Accelerometers," *IEEE Trans Nucl Sci* **43**: (6) 3127-3132 Part 1 Dec 1996.
25. A. R. Knudson, S. Buchner, P. McDonald, W. J. Stapor, A. B. Campbell, K. S. Grabowski, and D. L. Knies, "The Effects of Radiation on MEMS Accelerometers," *IEEE Trans Nucl Sci* **43**: (6) 3122-3126 Part 1 Dec 1996.
26. C. Pellet, M. Lecouve, H. Fremont A. Val, and D. Esteve, "Analysis of thermomechanical stresses in a 3D packaged micro electro mechanical system," *Microelectron Reliab* **38**: (6-8) 1261-1264 Jun-Aug 1998.
27. J. C. Forgrave, K. F. Man, and J. Mueller, "Finite Element Analysis of the Microisolation Valve," Proceeding of the MEMS Reliability and Qualification Workshop II, Pasadena, California, August 4-5, 1998.
28. J. A. Knapp, D. M. Follstaedt, S. M. Myers, J. C. Marbour, T. A. Friedmann, J. W. Ager, O. R. Monteiro and I. G. Brown, "Finite-element modeling of nanoindentation for evaluating mechanical properties of MEMS materials," *Surf Coat Tech* **104**: 268-275 May 1998.
29. F. Shi, P. Ramesh, and S Mukherjee, "Simulation Methods For Microelectromechanical Structures (MEMS) with Application to a Microtweezer," *Comput Struct* **56**: (5) 769-783 Sep 1995.
30. IntelliCAD, IntelliSense Corporation, Wilmington, MA.